

# Study on Application of Fisher Information for Power System Fault Detection

Shuping Cai<sup>a,b,\*</sup>, Guohai Liu<sup>b</sup>

<sup>a</sup>College of Electrical Information and Engineering, Jiangsu University, 212013 Zhenjiang, China;

<sup>b</sup>Key Laboratory of Facility Agriculture Measurement and Control Technology and Equipment of Machinery Industry, Jiangsu University, 212013 Zhenjiang, China

## Abstract

The ability to accurately detect power system faults is of vital importance for the purpose of isolating malfunctioning equipment and resuming normal operation as soon as possible after a fault occurs. People have used a variety of electric parameters as metrics to identify faults for a long time. The method proposed by this paper departs from the traditional approach by introducing Fisher information (FI) as a measure of the stability of electric signals and as a criterion for making fault decisions. In this way, a non-dimensional positive parameter is used as a single criterion to deliver fault detection for power distribution networks. Firstly, we simplified the formula of FI and then adopted a practical method for calculating values of FI. We demonstrated the application of FI to measure the stability of electric signals. Finally, we combined FI with wavelet analysis to propose a novel technique for phase selection of a power distribution network with a grounding short-circuit fault, namely the wavelet-based Fisher information (WFI). Simulation studies were then carried out to show the feasibility of the proposed method.

**Keywords:** Fisher Information; Power System; Fault Detection; Wavelet Analysis

## 1. Introduction

Security and stability have always been hot topics in power systems. Great efforts have been made over a long period of time to improve the operational reliability of power systems, triggering numerous research campaigns. However, traditional methods are now failing to achieve the desired results when used to improve the operational stability of the power system, as power distribution networks have greatly expanded and new-type electrical equipment have been installed. The precondition for boosting the level of stable operation of the power system is real-time monitoring and prediction [1, 2]. Thus, swift fault detection and accurate fault classification are very important elements when clearing faults and ensuring the safe and stable operation of a power distribution network.

Rapid advances in computer and automation technologies have opened the way for wide-ranging applications of intelligent devices such as electrical SCADA and Phase Measurement Units, Fault Information Systems and Transient Recorders. That has made it possible to obtain large quantities of a broad spectrum of measurement data in real time. This abundant real-time measurement data contains rich information that demonstrates the complexity and uncertainty

of the system, including fault information. This faithfully reflects real conditions of the system. By analyzing and synthesizing these conditions, we can then conclude whether the system is stable or secure at that time [3]. Thus the key is to find an appropriate criterion by which this vast array of measurement data can be fed into the decision-making process.

Fisher information is well known for its ability to measure the amount of information from measurements subject to uncertainties. The reason is that essentially any type of data or model can be converted into information regardless of disciplinary origin [4]. Unlike other measures of system information, Fisher information provides a method of monitoring system variables. Using this method, we can then monitor system states and state shifts [5]. The ability to detect states and state shifts permits the identification of fundamental changes occurring in the system and provides insight into what can be done to abate negative consequences [6]. In practice, Fisher information has been applied to derive fundamental equations of physics, thermodynamics and population genetics [7, 8]. More recently, ecologists have made far-reaching applications of Fisher information theory in ecological matters. Fath, Mayer et al. used it as a measure of dynamic order in complex systems [5, 9]. Mayer, Karunanithi et al. proposed it as a quantitative index for the detection and assessment of ecosystem regime shifts [9, 10] and as a sus-

\*Corresponding author

Email address: spcai@mail.ujs.edu.cn (Shuping Cai)

tainability metric [4]. Moreover, Fisher information has been used to study model systems including the stability of a multiple compartment food web [11, 12, 13] and to optimize control of dynamic model systems for sustainable environmental management [14, 15]. Rico-Ramirez et al. used Fisher information to assess dynamic models for therapeutic optimization in cancer immunotherapy and the continuous isothermal crystallization of ammonium sulfate [16]. The above reviews in rough terms the successful application of Fisher information theory in ecological areas. Inspired by this, this paper attempts to use it to detect faults in power systems.

One intrinsic property of Fisher information is that it is particularly suitable for detecting fundamental changes in a system, which makes it ideal for fault detection in systems such as distribution networks. Here, a first attempt is made to use it to address the problem of phase selection when a grounding short-circuit fault occurs in a distribution network. We also note that wavelet analysis is quite a useful technique for characterizing the local behavior of a signal subject to noise, in either time domain or frequency domain. Inspired by their respective merits, we propose a novel technique for phase selection of a power distribution network with a grounding short-circuit fault, namely wavelet-based Fisher information (WFI), which is designed to enhance the capabilities of Fisher information in terms of dealing with noise and uncertainties by exploring the power of wavelets.

The paper is organized as follows. Fisher information is introduced in Section II. Section III presents a practical method for computing wavelet-based Fisher information and then proposes a method for phase selection based on WFI. Simulation results are included in Section IV. Finally, we discuss the results in Section V.

## 2. Fisher information

Information theory provides a quantitative framework by which to describe processes that admit only partial knowledge [9]. In 1948 Shannon introduced the notion of entropy (also called Shannon entropy) as a measure of the amount of information in a signal source, which enriched its original meaning [3] and this is the origin of information entropy. In common with Shannon entropy, information entropy is a measure of the level of system uncertainties. For a signal source, the greater its information outputs, the greater its randomness and uncertainty. That is to say, its stability is very poor and accordingly its entropy value is very big. Information entropy, therefore, is regarded as a measure of the level of system disorder [17]. On the basis of information entropy, a number of variants of Shannon entropy have been introduced in the literature, for example, approximate entropy [18], which has been used to study the complexity of biological time series [19, 20], fault diagnosis of mechanical systems [19, 20, 21, 22] and electrical transmission systems [23], and wavelet entropy [24], which has found applications in fault detection in electrical distribution systems [25, 26] and electric power transient signal analysis as well [27, 28]

The statistician Ronald Fisher (Fisher 1922) developed a measure of indeterminacy, now called Fisher information. Fisher information can be interpreted as a measure of the ability to estimate a parameter, as the amount of information that can be extracted from a set of measurements, and also as a measure of the state of order or organization of a system or phenomenon [7]. Fisher information (FI) for a single measurement of one variable is calculated as follows:

$$FI = \int \frac{ds}{P(s)} \left( \frac{dP(s)}{ds} \right)^2 \quad (1)$$

where  $P(s)$  is the probability density function (PDF),  $s$  is a state variable.

Power system stability is conceptually associated with repeatability of observations. Hence, for a power system that is perfectly stable, repeated observations of the variables over time yield the same values within the limits of measurement uncertainty. Thus, for perfect stability, the probability density function ( $p(s)$ ) becomes a very sharp spike with derivative  $dp/ds$  that is approaching infinity and Fisher information (see Eq. 1) approaching infinity. This means that repeated measurements give increasingly more information eventually approaching infinite information. For a power system that is perfectly unstable, the opposite is true. Here all observations yield completely different and uncorrelated values for the variables, the likelihood of observing one value is the same as any other value, the probability density function ( $p(s)$ ) is flat, the derivative  $dp/ds$  is approaching zero and the Fisher information is near zero. Nevertheless real power systems exist between these two extremes of perfect stability and perfect instability and between infinite and zero Fisher information. Hence, Fisher information is a theoretically sound measure of power system stability. In practical application, in order to minimize calculation errors arising from dividing by small values of  $p(s)$ , we replace the probability density function in Eq. (1) with its amplitude, which is defined by  $q2(s) \equiv p(s)$ . Eq. (1) then becomes:

$$FI = 4 \int ds \left[ \frac{dq(s)}{ds} \right]^2 \quad (2)$$

Note that in specific calculation, we do not know the concrete form of the continuous function  $q(s)$ , but use instead a finite number of samples  $q_i$ . Thus Fisher information FI is usually computed numerically. For that purpose, we shall replace the derivative by the numerical difference ( $q_{i+1} - q_i$ ), and correspondingly use the sum of finitely many terms ( $q_{i+1} - q_i$ )<sup>2</sup> to approximate the integral, which then leads to the following formula for calculating Fisher information approximately:

$$I \approx 4 \sum [q_i - q_{i+1}]^2 \quad (3)$$

The expression in Eq. 3 will henceforth be used in all our Fisher information calculations.

## 3. Method

Signals occurring in an electrical distribution system are usually a combination of signals with various frequencies. In

normal operating conditions, the Fisher information of signals is not subject to significant changes. However, when a fault appears, the electrical distribution system will be running with a fault, and its currents and voltages will exhibit changes with characteristics which will be captured by the Fisher information. However, if we use the Fisher information directly for the analysis of faulty signals, it does not fully utilize the potential of Fisher information, since Fisher information is based on the derivative of the PDF, and thus it is more sensitive to local changes. It is well known that the technique of wavelet analysis is capable of capturing local changes in the frequency domain and time domain. If we process faulty signals using wavelet transform first, we obtain a set of coefficients which are sparse, meaning only a small portion of those coefficients will be significantly larger than zero, whereas the rest will be nearly zero. That is because most of the energy is contribute by a small portion of coefficients. This sparsity implies the distribution of the coefficients is much sharper in the middle than a Gaussian distribution, and has a clear tail towards the two ends [29]. These properties happen to be in good accordance with those of Fisher information based on the derivative of PDF. That inspires us to combine wavelet analysis with Fisher information; we thus propose wavelet Fisher information (WFI) for fault phase selection for electrical distribution networks.

Let the signal of concern  $x(n)$  be a time series. The wavelet decomposition of  $x(n)$  is as follows: the high-frequency coefficient and low-frequency coefficient at the  $k^{th}$  sample of the  $j^{th}$  decomposition are  $cD_j(k)$  and  $cA_j(k)$  respectively;  $D_j(k)$  and  $A_j(k)$  are the components after reconstruction, and the frequency bands covered by  $D_j(k)$  and  $A_j(k)$  are

$$cD_j(k) : [2^{-j}f_s, 2^{-(j-1)}f_s] \quad (4)$$

$$cA_j(k) : [0, 2^{-j}f_s] \quad j = 1, 2, \dots, J \quad (5)$$

where  $f_s$  is the sampling frequency and  $J$  is the maximum scale used in the wavelet decomposition. Then the original signal  $x(n)$  can be expressed as the sum of all components, i.e.,

$$\begin{aligned} x(n) &= D_1(n) + A_1(n) \\ &= D_1(n) + D_2(n) + A_2(n) \\ &= \dots = \sum_{j=1}^J D_j(n) + A_J(n) \end{aligned} \quad (6)$$

Finally let  $D_{j+1} = A_j$  and we have

$$x(n) = \sum_{j=1}^{j+1} D_j(n) \quad (7)$$

In the following we shall present the method for calculating Fisher information based on the above wavelet decomposition of the original signal  $x(n)$ . Suppose at the  $j^{th}$  scale, the

reconstructed component is  $D_j = \{d(1), \dots, d(N)\}$ . We then introduce a series of sliding windows  $W_m$  on  $D_j$ , as follows

$$W_m = \{d(k), \dots, d(k + w - 1)\} \quad (8)$$

where  $k = 1 + m \cdot \delta, w \in N$  is the window width,  $\delta \in N$  the sliding factor, and  $m = 1, \dots, M$  with  $M = (N - w)/\delta$  being the number of windows. Suppose all the elements in a sliding window  $W_m$  can be put into  $L$  bins. Then we have

$$Length(W_m) = \sum_{l=1}^L Length(Z_l) \quad (9)$$

where  $Length(\cdot)$  stands for the total number of data points contained in a window or bin of concern, and

$$Z_l = \{Z_l : |Z_l(i) - Z_l(j)| \leq 3 * \sigma; i, j \leq 1, 2, \dots, w; i \neq j\} \quad (10)$$

Namely, the total number of elements in a sliding window equals the sum of the subtotals contained in those bins. Note that here  $\sigma$  is the standard deviation of the component  $D_j$  for normal phases. According to Chebyshev's theorem, the above binning process guarantees that 89 of the data points in this window fall into the same bin, irrespective of the probability distribution. We summarize the procedures involved in the binning method: (i) categorize a time series (i.e., the discrete wavelet component) into a sequence of time windows, (ii) in each window convert data points into states by using the above method, (iii) in each window construct a probability distribution function for possible states of the system, and (iv) compute the Fisher information from the PDFs constructed in (iii).

## 4. Results

### 4.1. Measurement of stability for ideal electric signals

We constructed the following four ideal electric signals:

$$S_1 = \sin(2\pi f_1 t)$$

$$S_2 = 0.5\sin(2\pi f_1 t) + 0.5\sin(2\pi f_2 t)$$

$$S_3 = 0.25\sin(2\pi f_1 t) + 0.25\sin(2\pi f_2 t) + 0.25\sin(2\pi f_3 t) + 0.25\sin(2\pi f_4 t)$$

$$S_4 = \sin(2\pi f_1 t) + N.$$

Where  $f_1 = 50$  Hz,  $f_2 = 150$  Hz,  $f_3 = 250$  Hz,  $f_4 = 350$  Hz;  $N$  is a zero mean white noise source.

From the above four signals, real-time data are collected for 2000 points with a 0.05 second interval and a sampling rate of 20 kHz, respectively. Note that here we only use Fisher information (namely Eq. 3) to measure the level of stability of all four signals and do not involve any wavelet transforms.

Fig. 1 shows their corresponding waveforms. Finally, we used the proposed binning method to calculate the values of Fisher information for every signal; they are shown in Table 1 below.

As shown in Table 1,  $S_4$  has the most smallest FI value of the four signals. That is because  $S_4$  contains a white noise source, which makes it more unstable, whereas the other three signals have the same and the biggest FI values due

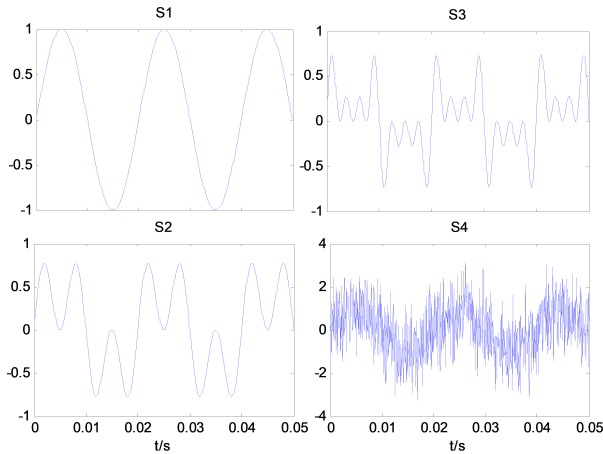


Figure 1: Four ideal electric signals waveforms

Table 1: FI of four ideal electric signals

Signal	$S_1$	$S_2$	$S_3$	$S_4$
FI	4	4	4	1.3069

to their stability and periodicity. The FI value is clearly closely related to the stability of the signals. Namely, the greater the instability of a signal is, the smaller its FI value is, which is as expected.

We altered the amplitude of the above four signals to see whether their FI values would be subject to such change. Table 2 shows the test results.

We can see clearly that FI values in Table 2 are almost the same as in Table 1. The only difference is that the FI value calculated by signal  $S_4$  is slightly different to the one calculated by signal  $0.5 S_4$ . This is because the white noise signal that  $S_4$  and  $0.5 S_4$  contain is generated randomly, which will have a marginal effect on the calculation of FI values. This situation does not lead to any changes as regards the conclusion drawn from the testing, which is that the FI value of a signal is unrelated to its amplitude.

Finally, we investigated another situation. Namely, we altered the proportion of white noise a signal contains, i.e., the noise-to-signal ratio (NSR), to see the effect on the FI of the signal.

As shown in table 3, the FI of the signal increases as its NSR falls gradually. When its NSR is reduced to a certain degree, the FI of the signal is the same as for stable signals. So the proposed method based on Fisher information has a certain ability to restrain noise.

In summary, the FI based method is able to distinguish exactly between stable signals and unstable ones when used to analyze electric signals. Moreover, the result of the analysis

Table 2: FI of signals with different magnitude

Signal	$0.1 S_1$	$5 S_2$	$10 S_3$	$0.5 S_4$
FI	4	4	4	1.3326

Signal	$S_1 + 0.1N$	$S_1 + 0.1N$	$S_1 + 0.1N$
FI	2.3135	3.9563	4

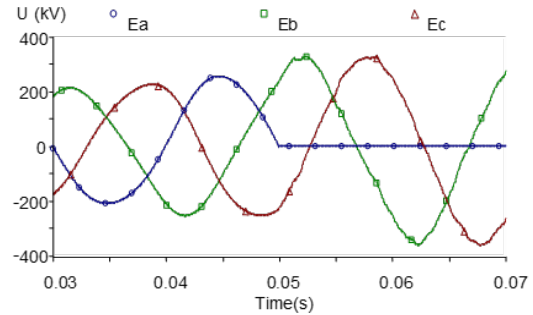


Figure 2: Voltage waveforms of single-phase grounding fault

presented by the method is unaffected by the amplitude of the signals. In addition, it has a certain anti-noise capability.

#### 4.2. Phase selection for power distribution networks with grounding faults

PSCAD/EMTDC power system simulation software was used to set up the simulation model of a 500 kV Dual-power supply distribution network. The positive-sequence parameters are

$r_1 = 0.0363 \Omega/\text{km}$ ,  $x_1 = 0.286 \Omega/\text{km}$ ,  $b_1 = 3.425 \times 10^{-6} \text{ S/km}$ , and the zero-sequence parameters are  $r_0 = 0.379 \Omega/\text{km}$ ,  $x_0 = 1.021 \Omega/\text{km}$ ,  $b_0 = 4.767 \text{ S/km}$ , where the length of the transmission line is 180 km.

Three scenarios were simulated, including single-phase grounding fault, two-phase grounding fault and three-phase grounding fault. Let us suppose that grounding faults occur at  $t=0.05\text{s}$ . The analysis is focuses mainly on the voltages of all three phases. Real-time data are collected for two cycles, one before the fault onset and one afterwards, with a sampling rate of 20 kHz. The collected data are then decomposed by using db5 wavelets. Finally, we calculated the values of the wavelet-based Fisher information of the voltages for every phase, by applying the proposed binning method to the coefficients  $D_2(n)$ .

Fig. 2 shows the waveforms of the voltages of all three phases when an A-phase grounding fault occurs. As shown in Fig. 2, all the voltages of the three phases are quite normal, and all of them exhibit sinusoidal waveform before the fault onset, which is quite reasonable since the network has a symmetric topology and no fault has occurred yet within the network. However, all the voltages start to deviate from initial values as soon as the fault happens (at  $t = 0.05 \text{ s}$ ), which means the fault has changed the overall behavior of the network. What is more interesting is the difference between the voltages of normal phases and that of the faulty phase. In fact, following the fault, the voltage of faulty phase A drops to zero instantly, then those of normal phases B and

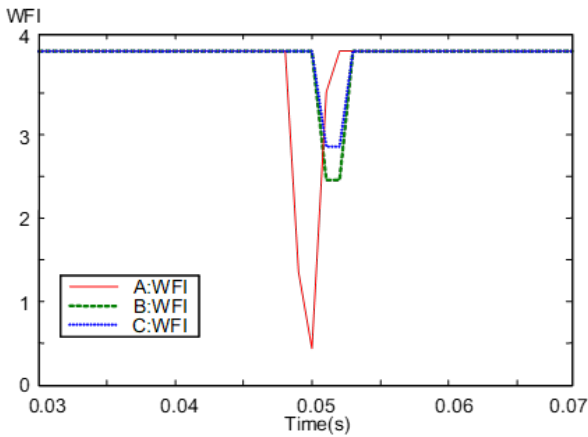


Figure 3: WFI of faulty phase A and normal phases

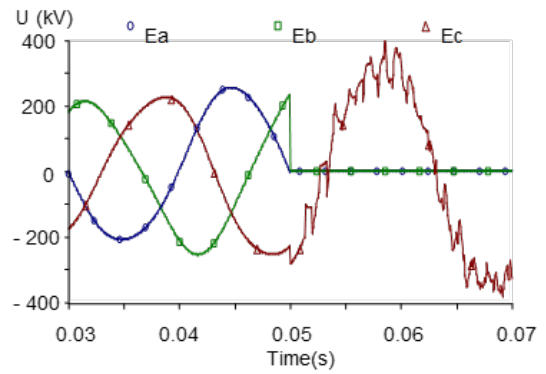


Figure 4: WFI of fault phase A and normal phases

C go up, which is quite different. This observation is essential for phase selection, as it implies that there are fundamental differences between the voltages of normal phases and that of the faulty phase. Despite all this, one should not expect to base phase selection on a visual inspection of those voltages, because real running conditions may be much more complex than the ideal one. More importantly, we need a more robust trigger signal to activate safety protection devices to rapidly isolate faulty equipment after a fault happens. That is why we proposed this phase selection method based on the WFI, as it can cope reasonably well with noise.

The WFI obtained based on wavelet decomposition is shown in Fig. 3. Prior to the onset of the fault, the WFI of the voltages of all three phases remained at the same level (around 4), which is again expected since there is no fault in the network. Then the WFI values of all three phases mark a step change when the fault happens. However the level of changes is different for those three phases—the faulty phase has the most significant change of the three phases. That is because when a single-phase grounding fault occurs, the voltage of the faulty phase contains more information about the fault than the other two normal phases, and thus the WFI of the faulty phase should exhibit more deviation from the fault-free WFI. Moreover, at the time of occurrence of the step change of the two normal phases the WFI lags behind that of the faulty one, which characterizes the causal relationship between the faulty phase and the normal phases when there is a single-phase grounding fault. Hence the results in Fig. 3 show that the proposed method based on WFI can identify the faulty phase well, in terms of amplitude and time.

Consider the second scenario, where a two-phase grounding fault occurs at  $t = 0.05$  s. The waveforms of the voltages of all three phases are shown in Fig. 4. Comparing to Fig. 1, although this is a different fault scenario, a similar pattern is evident: there is a significant difference between the voltage of normal phase C and those of the other two faulty phases. The WFI values of the voltages in the above scenario are shown in Fig. 5. It can be clearly seen that the conditions of this fault scenario are quite different from those of the previ-

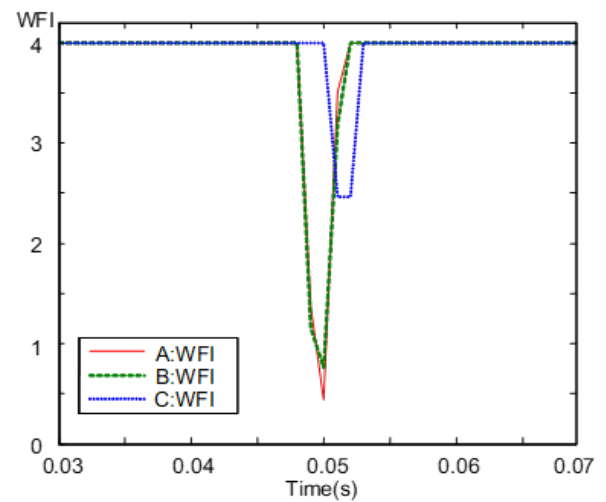


Figure 5: WFI of fault phase A and normal phases

ous one, yet the distinct characteristics of the faulty phases still stand out.

The third simulation investigates the case of a three-phase grounding fault happening at  $t = 0.05$  s. Note that in this case, the waveforms of the voltages of all three phases are almost identical after the fault occurs, as shown in Fig. 6, since the parameters of those three phases are exactly the same, and so this is completely understandable. The WFI values are plotted in Fig. 7. As expected, the WFI values of all three phases have nearly the same changes.

The simulated results above share a common characteristic. Namely, the WFI of all three phases have an obvious abrupt change when the fault happens, and the level of the abrupt changes of the faulty phase WFI is much bigger than that of the normal ones.

For every type of failure above, the WFI values of all three phases at the bottom of the abrupt change are recorded in Table 4. As shown in Table 4, the WFI values of the faulty phases are significantly lower than for the normal phases at the bottom. Consequently, we can identify faulty phases by comparing the WFI values of all three phases at the bottom.

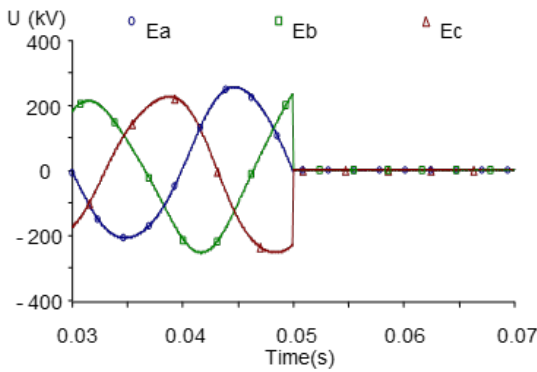


Figure 6: Voltage waveforms of three-phase grounding fault

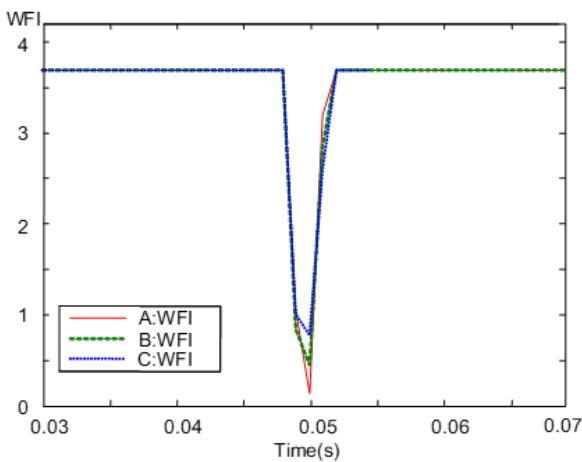


Figure 7: WFI of all three fault phases

The question is whether the stability of the signals measured by the proposed method is subject to their amplitudes. This can be answered by reference to Table 2. The table shows that the stability of the signals measured by the method is independent of their amplitudes, which means this proposed method is especially suitable to detect small signals. Table 3 shows that the WFI values of the signals increases gradually as their uncertainties reduce. The reverse is also true. Moreover, for those signals containing a little noise, their WFI values stay roughly the same, which means the method can cope with noise.

Fig. 3 shows the WFI value of faulty phase A undergoes a series of changes when a single-phase grounding fault occurs. Namely, the value suddenly drops to 0.4389 the moment the fault happens ( $t = 0.05$  s) from 4, which is the WFI value when the network has no fault, and then rapidly jumps up to 4 once again, as noted in the first row in Table 4. Physically, this process characterizes the whole course of the occurrence of the faults. We can also see from Fig. 3 that normal phases B and C experience the same process as well, yet the intensity of the changes of their WFI values is much lower than for the faulty one. It is worth noting that the abrupt changes seen in the WFI of normal phases B and C are slightly different. That is because that at the time the fault occurs, the fault characteristics associated with these two normal phases is not exactly identical. However, that does not affect the ultimate outcome of phase selection. Interestingly, there is a time delay between the abrupt changes in faulty phase WFI and those of normal phases WFI, which reflects the relationship between the causes and the consequences when the fault appears.

### 5. Discussion

Fisher information, an important method in information theory, was originally developed as a measure of the information content in data. We introduced it into a power system and then applied it to measure the stability of the electrical signals and to detect faults in distribution networks.

As shown in Table 1  $S_1$  is a signal with a single frequency.  $S_2$  and  $S_3$  are a combination of signals of various frequencies. All of them are stable signals, so their WFI values have the maximum value 4. However,  $S_4$  contains noise, which makes it more unstable. Thus its WFI value is only 1.3069.

Table 4: WFI values of all three phases at the bottom for every type of failure

Faulty type	phases	WFI
A phase fault	A	0.4389
	B	2.851
	C	2.456
A and B phases fault	A	0.4389
	B	0.7573
	C	2.456
AB and C phases fault	A	0.4389
	B	0.7573
	C	1.082

Fig. 5 demonstrates the evolution of the WFI values of all three phases when a two-phase grounding fault occurs. See also from the second row in table IV, the WFI values of two fault phases drop to the minimum values 0.4389 and 0.7573 respectively at the time the fault happens ( $t = 0.05$  s). It is worth noting that these values differ slightly. That is because at the time the fault occurs, the fault characteristics associated with these two faulty phases is not exactly identical. Normal phase C has a similar process compared to the above faulty phases, but its WFI value is 2.456 at the bottom, which is much bigger than that of the faulty phases. Moreover, there is also a time delay between the abrupt changes of the two faulty phases WFI and that of the normal phase WFI. When a three-phase grounding fault happens, the WFI values of voltages of all three phases show nearly the same pattern, provided the three phases have the same parameters. This case is shown by Fig. 7. The WFI values of three faulty phases drop to the minimum values of 0.4389, 0.7573 and 1.082 respectively at the time the fault happens ( $t = 0.05$  s); see in particular the third row in table IV. The difference among them is not very big, which enables us to conclude that it is a three-phase grounding fault.

## 6. Conclusion

This paper first introduces Fisher information as a measure of the stability of electric signals then we combine it with wavelet analysis to tackle phase selection in a power distribution network with a grounding short-circuit fault.

Simulation results have shown that this method can differentiate with exactitude the level of stability of varieties of the signals, and the obtained result is unaffected by the amplitude of the signals. What's more, it has a certain anti-noise capability. Fisher information based on wavelet analysis can quantitatively distinguish faulty phases from non-faulty ones, under varied conditions such as single-phase grounding fault, two-phase grounding fault and three-phase grounding fault. The method can also identify when a fault occurs.

## References

- [1] B. Ingelsson, P.-O. Lindstrom, D. Karlsson, G. Runvik, J.-O. Sjodin, Wide-area protection against voltage collapse, *IEEE Computer Applications in Power* 10 (4) (1997) 30–35.
- [2] J. Hauer, D. Trudnowski, G. Rogers, B. Mittelstadt, Keeping an eye on power system dynamics, *IEEE Computer Applications in Power* 10 (4) (1997) 50–54.
- [3] W. Yang, Application prospects of entropy theory in power systems, *Power Construction* (3) (2000) 17–19.
- [4] H. Cabezas, B. D. Fath, Towards a theory of sustainable systems, *Fluid Phase Equilibria* 194 (01) (2002) 3–14.
- [5] B. D. Fath, H. Cabezas, C. W. Pawlowski, Regime changes in ecological systems: an information theory approach, *Journal of Theoretical Biology* 222 (4) (2003) 517–530.
- [6] T. Eason, H. Cabezas, Evaluating the sustainability of a regional system using fisher information in the san luis basin, colorado, *Journal of Environmental Management* 94 (1) (2012) 41–49.
- [7] B. R. Frieden, P. M. Binder, *Physics from Fisher Information: A Unification*, Cambridge University Press, 2004.
- [8] A. K. Evans, Book review: Probability, statistical optics and data testing. b.r. Frieden, third edition, springer, berlin, 2001., *Optics and Lasers in Engineering* 38 (5) (2002) 319–320.
- [9] A. L. Mayer, C. W. Pawlowski, H. Cabezas, Fisher information and dynamic regime changes in ecological systems, *Ecological Modelling* 195 (1) (2006) 72–82.
- [10] A. T. Karunanithi, H. Cabezas, B. R. Frieden, C. W. Pawlowski, Detection and assessment of ecosystem regime shifts from fisher information, *Ecology and Society* 13 (1) (2008) 439–461.
- [11] B. D. Fath, H. Cabezas, Exergy and fisher information as ecological indices, *Ecological Modelling* 174 (1) (2004) 25–35.
- [12] H. Cabezas, C. W. Pawlowski, A. L. Mayer, N. T. Hoagland, Sustainable systems theory: ecological and other aspects, *Journal of Cleaner Production* 13 (5) (2005) 455–467.
- [13] H. Cabezas, C. W. Pawlowski, A. L. Mayer, N. T. Hoagland, Simulated experiments with complex sustainable systems: Ecology and technology, *Resources Conservation and Recycling* 44 (3) (2005) 279–291.
- [14] Y. Shastri, U. Diwekar, H. Cabezas, J. Williamson, Is sustainability achievable? exploring the limits of sustainability with model systems., *Environmental Science and Technology* 42 (17) (2008) 6710–6716.
- [15] Y. Shastri, U. Diwekar, H. Cabezas, Optimal control theory for sustainable environmental management, *Environmental Science and Technology* 42 (14) (2008) 5322.
- [16] V. Rico-Ramirez, P. A. Quintana-Hernandez, J. A. Ortiz-Cruz, S. Hernandez-Castro, Fisher information: A generalized sustainability index?, *Computer Aided Chemical Engineering* 25 (08) (2008) 1155–1160.
- [17] I. A. Rezek, S. J. Roberts, Stochastic complexity measures for physiological signal analysis., *IEEE transactions on bio-medical engineering* 45 (9) (1998) 1186–91.
- [18] P. SM, Approximate entropy as a measure of system complexity., *Proceedings of the National Academy of Sciences of the United States of America* 88 (6) (1991) 2297–2301.
- [19] Z. Jiang, H. Feng, D. Liu, T. Wang, [analyzing sleep eeg using correlation dimension and approximate entropy], *Journal of Biomedical Engineering* 22 (4) (2005) 649.
- [20] Z. Nan, X. Liu, S. Wang, M. Wan, L. Fei, Dynamic complexity analysis to cognitive event-related potential based on tsallis entropy and approximate entropy, *Journal of Xian Jiaotong University* 41 (2) (2007) 245.
- [21] X. U. Yong, Approximate entropy and its applications in mechanical fault diagnosis, *Information and Control* 31 (6) (2002) 547–551.
- [22] H. Hu, X. Ma, Application of local wave approximate entropy in mechanical fault diagnosis, *Journal of Vibration and Shock*.
- [23] F. U. Ling, H. E. Zheng-You, R. K. Mai, Q. Q. Qian, Application of approximate entropy to fault signal analysis in electric power system, *Proceedings of the Csee* 28 (28) (2008) 68–73.
- [24] S. Blanco, A. Figliola, R. Q. Quiroga, O. A. Rosso, E. Serrano, Time-frequency analysis of electroencephalogram series. iii. wavelet packets and information cost function, *Physical Review E Statistical Physics Plasmas Fluids and Related Interdisciplinary Topics* 51 (3) (1998) 2624.
- [25] Z. Y. He, Y. M. Cai, Q. Q. Qian, Study of wavelet entropy theory and its application in electric power system fault detection, *Proceedings of the Csee*.
- [26] H. Zheng-you, L. Zhi-gang, Q. Qing-quan, Study on wavelet entropy theory and adaptability of its application in power system, *Power System Technology* 32 (32) (2004) 913–20.
- [27] X. Q. Chen, H. E. Zheng-You, F. U. Ling, Electric power transient signals classification and recognition method based on wavelet energy spectrum, *Power System Technology* 30 (17) (2006) 59–63.
- [28] H. E. Zheng-You, G. M. Luo, J. W. Yang, Power transients recognition based on wavelet energy matrixes similarity, *Journal of Electric Power Science and Technology*.
- [29] S. Mallat, A theory for multiresolution signal decomposition: The wavelet representation, *IEEE Transactions on Pattern Analysis and Machine Intelligence* 11 (7) (1989) 674–693.